ACS Macro Letters

pubs.acs.org/macroletters Letter

Oxygen Tolerance during Surface-Initiated Photo-ATRP: Tips and Tricks for Making Brushes under Environmental Conditions

Gianluca Gazzola, Irene Filipucci, Andrea Rossa, Krzysztof Matyjaszewski,* Francesca Lorandi,* and Edmondo M. Benetti*

Cite This: *ACS Macro Lett.* 2023, 12, 1166–1172 Read Online

ACCESS | Metrics & More | Article Recommendations | Supporting Information

ABSTRACT: Achieving tolerance toward oxygen during surface-initiated reversible deactivation radical polymerization (SI-RDRP) holds the potential to translate the fabrication of polymer brush-coatings into upscalable and technologically relevant processes for functionalizing materials. While focusing on surface-initiated photoinduced atom transfer radical polymerization (SI-photoATRP), we demonstrate that a judicious tuning of the composition of reaction mixtures and the adjustment of the polymerization setup enable to maximize the compatibility of this grafting technique toward environmental conditions. Typically, the presence of O_2 in the polymerization medium limits the attainable thickness of polymer brushes and causes the occurrence of "edge effects", *i.e.*, areas at the substrates' edges where continuous oxygen diffusion from the surrounding environment inhibits brush growth. However, the concentrations of the Cu-based catalyst and "free" alkyl halide initiator in solution emerge as key parameters to achieve a more efficient consumption of oxygen and yield uniform and thick brushes, even for polymerization mixtures that are more exposed to air. Precise variation of reaction conditions thus allows us to identify those variables that become determinants for making the synthesis of brushes more tolerant toward oxygen, and consequently more practical and upscalable.

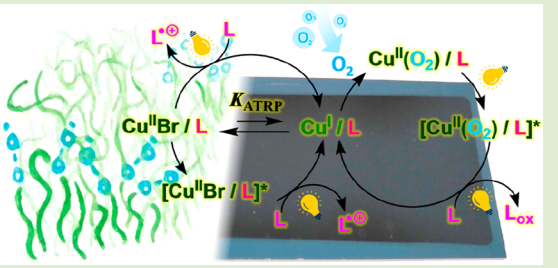

The development of reversible deactivation radical polymerization (RDRP) methods that show high tolerance toward environmental conditions has triggered intense efforts in establishing parallel processes for the fabrication of polymer brushes exploiting the corresponding surface-initiated polymerization (SI-P) techniques.[1−4] The past decade of research in this subfield of polymer chemistry has aimed to provide robust and upscalable SI-RDRPs to yield brushes over large substrates while using comparatively small volumes of polymerization solutions and without the need for degassing the mixtures and using inert atmospheres. If these conditions were fully accomplished, the modification of technologically relevant substrates (*e.g.*, polymer films for packaging[5] or supports for biotechnological applications[6]) by using polymer brushes would be enabled, and the translation of SI-RDRP into an industrially upscalable process could be realistically foreseen.

Especially concentrating on surface-initiated atom transfer radical polymerization (SI-ATRP) methods,[7] tolerance to oxygen has been achieved by means of reducing agents that regenerate the catalyst inactivated by recombination with oxygen, during surface-initiated activators regenerated by electron transfer ATRP (SI-ARGET ATRP).[5,8−11] Alternatively, zerovalent metals such as Cu^0,[12−17] Fe^0,[18] or Zn^0[19] can act as oxygen scavengers within small reaction volumes, or enzymes can be exploited to consume oxygen through reaction paths that are independent of the SI-ATRP.[20]

Surface-initiated photoinduced ATRP (SI-photoATRP) represents an alternative to these methods. SI-photoATRP enables to generate brushes without the need for preliminary degassing of reaction mixtures, by sandwiching microliter volumes of polymerization solution between initiator-functionalized substrates and a glass slide and irradiating this simple setup with UV light in air.[7,21] Similar to the corresponding case of photoATRP performed in solution, during SI-photoATRP, the synergistic effect of an excess of ligand (L), serving as reducing agent, and UV light, providing Cu^{II} species in a photoexcited state, enables the continuous regeneration of Cu^{I}/L-based activators from X-Cu^{II}/L deactivators (X = Br, Cl) and $Cu^{II}(O_2)$/L complexes, thus simultaneously consuming oxygen in the reaction medium (Figure 1).[21−23]

However, whereas photoATRP in solution requires closed vessels and the absence of air-filled headspace to become tolerant to the oxygen dissolved in the medium,[24] SI-photoATRP can be performed under open-air conditions, due to the limited amount of O_2 diffusing into the reaction

Received: June 12, 2023
Accepted: July 26, 2023
Published: August 1, 2023

https://doi.org/10.1021/acsmacrolett.3c00359
ACS Macro Lett. 2023, 12, 1166−1172

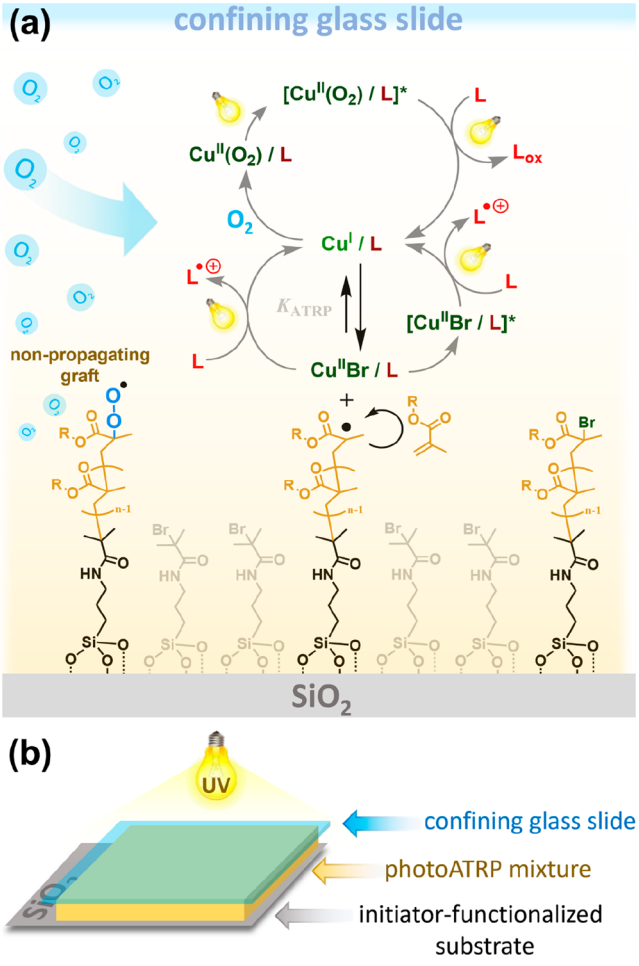

Figure 1. (a) Mechanism of SI-photoATRP highlighting oxygen consumption by recombination with Cu^I/L catalyst and termination of propagating grafts by reaction with O_2 diffusing from the edges of the polymerization setup. (b) The typical SI-photoATRP setup used in this study.

volume through the sides of the polymerization setup (Figure 1).[21,25,26]

Diffusion of O_2 and its consumption by the phototriggered process underlying SI-photoATRP are in competition and determine the occurrence of "edge effect" on brush films, *i.e.*, the presence of areas at the substrates' edges where brush growth is inhibited by diffusing oxygen.[25,27] The width of such areas (d_{edge}) provides a direct indication of the capability of the SI-photoATRP system. By analogy to photoATRP in solution, d_{edge} thus correlates to the induction period that is necessary for the consumption of O_2 by the components of the polymerization mixture. When O_2 consumption is more efficient, the induction period of a polymerization in solution is shorter, which corresponds to a lower d_{edge} for surface-initiated polymerizations.

Since the technological potential of SI-photoATRP strongly depends on its tolerance to oxygen,[5,27] it becomes fundamentally important to assess which parameters influence the brush thickness, formation of edges, and their extension across substrates when no degassing is applied, and the polymerization is not conducted within an inert environment.

In this work, the growth and homogeneity of brushes are evaluated while varying the type of ligand for the Cu catalyst, its concentration, the polymerization volume above the initiator-bearing substrate (*i.e.*, degree of confinement), and the presence/concentration of "free" ATRP initiator in solution.

Besides the effects of the ligand and "free" initiator, recently identified among the main factors determining the insusceptibility of solution photoATRP toward oxygen,[28] this research highlights how additional features distinctive of a surface-initiated process can be exploited as tools to modulate its tolerance to ambient conditions (hence its applicability within technologically relevant settings).

SI-photoATRP was performed within an extremely accessible setup, which is schematized in Figure 1b. A 1 μL cm^{-2} polymerization mixture was poured on an ATRP initiator-functionalized SiO_x substrate, which was subsequently covered by a borosilicate glass slide and finally irradiated with UV light (λ_{max} = 365 nm) for the desired time. Typical polymerization mixtures comprised oligo(ethylene glycol)methacrylate (OEGMA) as monomer (M_n ~ 300 and 500 Da), dimethylformamide (DMF) as solvent (OEGMA:DMF 50:50 v/v), Cu^IIBr_2/L and free ligand.

Ligand plays a critical role in the oxygen tolerance of photoATRP, as it regulates the regeneration of activators (Cu^I/L), by acting as electron donor for both the photoexcited [Br–Cu^II/L]* species and the superoxide Cu complex $Cu^II(O_2)$/L.[22,29−32] The latter forms upon reaction between Cu^I-based species and molecular oxygen.[21,33] SI-photoATRP of OEGMA was conducted by testing two different ligands, namely, tris(2-dimethylaminoethyl)amine (Me_6TREN) and tris(2-pyridylmethyl)amine (TPMA) (while keeping [$CuBr_2$]:[L] = 1:6). When [$CuBr_2$] was set at 1 mM, thicker POEGMA brushes were grown with L = Me_6TREN compared to those synthesized with L = TPMA after 1 h of polymerization, reaching a brush dry thickness (T_{dry}) of 106 ± 2 and 48 ± 4

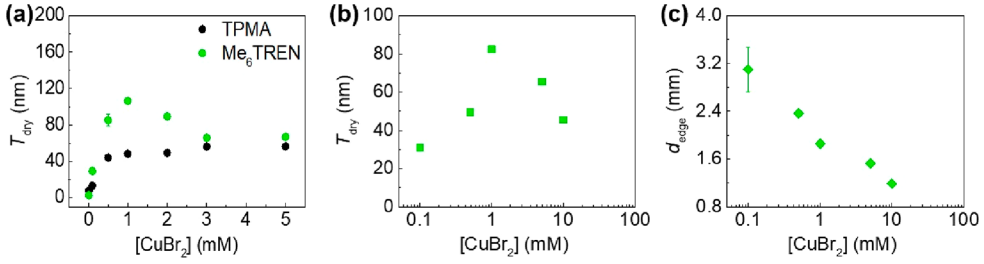

Figure 2. (a) Dry thickness (T_{dry}) for SI-photoATRP of OEGMA (M_n ~ 500 Da) carried out for 1 h in polymerization mixtures comprising 1:1 (v/v) DMF:OEGMA and different concentrations of $CuBr_2$, using TPMA (black dots) and Me_6TREN (green dots) as ligands (L) in a ratio [$CuBr_2$]:[L] of 1:6. (b, c) Dry thickness (T_{dry}) and edge distance (d_{edge}) for SI-photoATRP of OEGMA (M_n ~ 300 Da) carried out in polymerization mixtures comprising 1:1 (v/v) DMF:OEGMA and different concentrations of $CuBr_2$, using Me_6TREN as ligands (L) in a ratio [$CuBr_2$]:[L] of 1:6.

https://doi.org/10.1021/acsmacrolett.3c00359
ACS Macro Lett. 2023, 12, 1166−1172

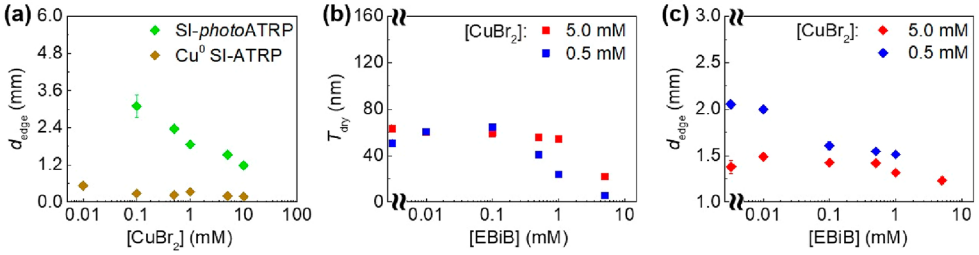

Figure 3. (a) Comparison of the edge distance (d_{edge}) measured on brush-functionalized substrates upon SI-photoATRP and Cu^0-mediated SI-ATRP of OEGMA ($M_n \sim 300$ Da) carried out in polymerization mixtures comprising 1:1 (v/v) DMF:OEGMA and different concentrations of $CuBr_2$, using Me_6TREN as the ligand (L) in a ratio $[CuBr_2]$:[L] of 1:6 for SI-photoATRP (green points) and at a constant concentration for Cu^0-mediated SI-ATRP (20 mM, brown points). (b, c) Dry thickness (T_{dry}) and (d) edge distance (d_{edge}) for SI-photoATRP of OEGMA ($M_n \sim 300$ Da) carried out in polymerization mixtures comprising 1:1 (v/v) DMF:OEGMA, $CuBr_2$ = 5 mM (red points) and 0.5 mM (blue points), and using Me_6TREN as the ligand (L) in a ratio $[CuBr_2]$:[L] of 1:6, with different concentrations of EBiB as the sacrificial initiator.

nm, respectively (Figure 2a). A faster growth of POEGMA brushes could be attributed to the higher ATRP activity of Cu/Me_6TREN compared to Cu/TPMA, and to the higher efficacy of Me_6TREN as electron donor compared to TPMA (Figure S4).[34] When $[Cu^{II}Br_2/Me_6TREN]$ was varied from 0.1 to 5 mM, T_{dry} increased to 106 ± 2 nm, until copper concentration reached 1 mM, and then decreased, leveling off to a $T_{dry} \sim 65$ nm at $[Cu^{II}Br_2/ Me_6TREN] \geq 3$ mM. In contrast, when L = TPMA, T_{dry} progressively increased with increasing $[Cu^{II}Br_2/TPMA]$, until reaching a plateau at $T_{dry} \sim 56$ nm for $[Cu^{II}Br_2/TPMA] \geq 2$ mM.

We believe that the overall different dependences of T_{dry} on $[Cu^{II}Br_2/L]$ while comparing L = TPMA and Me_6TREN were mainly due to a combination of the diverse effectiveness of the two species to act as electron donors and the distinctive K_{ATRP} characterizing the corresponding Cu-based catalysts. For $0 \leq [Cu^{II}Br_2/L] \leq 1$ mM, the increment in POEGMA brush growth is more significant while using Me_6TREN rather than TPMA. However, a further increase in $[Cu^{II}Br_2/Me_6TREN]$ beyond 1 mM led to accumulation of deactivator, which determined a progressive slowing down of polymerization.[16] This phenomenon was particularly evident in the case of L = Me_6TREN due to the higher K_{ATRP} for the corresponding Cu catalyst relative to the TPMA-based analogues, which results in higher deactivator concentration and, thus, in a T_{dry} versus $[CuBr_2]$ profile showing a maximum.[16]

It is also important to emphasize that while the type of ligand influenced T_{dry}, a significant impact on d_{edge} could not be observed (Figure S5).

In contrast, the brush growth rate and the tolerance of SI-photoATRP toward O_2 were significantly affected by the concentration of $CuBr_2$/L. While keeping a polymerization time of 60 min, T_{dry} showed a marked increment with increasing $[CuBr_2/Me_6TREN]$ until a concentration of 1 mM was reached (Figure 2b). A further increment in $[CuBr_2/Me_6TREN]$ was mirrored by a progressive decrease of T_{dry}, presumably due to the accumulation of deactivator species that slowed down SI-photoATRP.[16,21] Simultaneously, upon increasing $[CuBr_2/Me_6TREN]$ from 0.01 to 10 mM, a progressive and monotonic decrease in d_{edge} from 3.1 ± 0.4 to 1.2 ± 0.1 mm was recorded (Figures 2c and S6), indicating that an increased catalyst loading facilitated oxygen scavenging and enabled the fabrication of brush films with more uniform morphology across the entire substrate. This finding was in good agreement with previous results by the group of Hawker, which highlighted how the efficiency of oxygen consumption could be improved by incrementing the phenothiazine (PTH)-based catalyst loading during metal-free SI-photoATRP.[25,26] In a similar way, an increment in the content of Cu-based catalyst provided a faster complexation of O_2 diffusing from the surrounding environment and its subsequent consumption through the photoATRP process (Figure 1), leading to a reduction in the areas where brush growth is inhibited at the substrate's edges. It is important to emphasize that when $[CuBr_2/Me_6TREN] > 1$ mM improved oxygen tolerance was gained at the expense of the polymerization rate, suggesting that the catalyst content should be carefully adjusted to achieve the best compromise between brush thickness and homogeneity.

Interestingly, catalyst content has a significantly different effect on oxygen tolerance while comparing SI-photoATRP and SI-ATRP mediated by Cu^0 plates (Cu^0 SI-ATRP), which was highlighted as one of the most efficient techniques to fabricate brushes under environmental conditions.[17] The mechanism of Cu^0 SI-ATRP is strongly affected by the different components of the polymerization mixture (which is generally not deoxygenated), also including O_2. The latter is rapidly consumed through the formation of a CuO_x layer on the Cu^0 surface, which contributes to the generation of soluble Cu^I/Cu^{II} species when free ligand is present in solution.[15] We previously reported that during Cu^0 SI-ATRP the presence of oxygen inhibited brush growth only in the proximity of substrates' edges.[16] Herein, we compared the values of d_{edge} in Cu^0 SI-ATRP and SI-photoATRP when these were performed under similar reaction conditions. Relevantly, the values of d_{edge} were visibly much smaller when POEGMA brushes were synthesized by Cu^0 SI-ATRP with respect to analogous films obtained through the corresponding photochemical process (Figure 3a). Also, for Cu^0 SI-ATRP, d_{edge} tended to increase with decreasing $[CuBr_2]$, albeit to a significantly lower extent.

Hence, if d_{edge} for a SI-ATRP process in the presence of O_2 is associated with an induction period for the solution polymerization counterpart, then under similar conditions Cu^0-mediated ATRP should result in shorter induction periods than those typical of the UV light-mediated analogue (although a comparative analysis for the two different solution processes has not been conducted). While focusing on surface-initiated techniques, our experiments suggest that the presence of a Cu^0 plate promotes a more effective consumption of oxygen, which is also less affected by the composition of the polymerization mixture, in comparison to SI-photoATRP systems.

In addition to the catalyst content, the concentration of alkyl halide initiator (RX) was identified as one of the main

https://doi.org/10.1021/acsmacrolett.3c00359
ACS Macro Lett. 2023, 12, 1166−1172

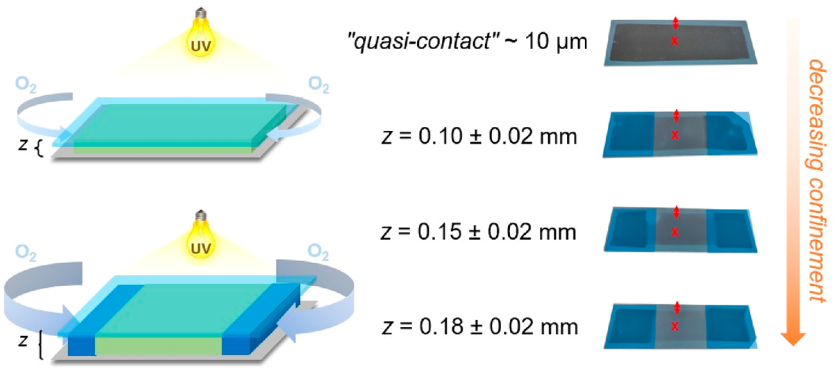

Figure 4. Experimental setup for the study of the confinement effect. The regions occupied by the spacers were covered with partly transparent blue squares as a guide for the eyes.

determinants for oxygen consumption during photoATRP in solution.[28] Typical SI-photoATRP do not necessarily require the presence of an initiator in solution (which would act as a sacrificial initiator).[21] However, this was often employed during "normal" SI-ATRP to increase the concentration of Cu^{II}-based deactivators in polymerization mixtures and provide an estimate of the molar mass of the surface-grafted polymer,[35−37] or to increase the viscosity of the reaction medium.[38]

In order to test the contribution of the free initiator to the oxygen tolerance of SI-photoATRP, the values of T_{dry} and d_{edge} were recorded while varying the concentration of ethyl α-bromoisobutyrate (EBiB) within a polymerization mixture with otherwise constant [$CuBr_2$/Me_6TREN] = 5 mM (Figure 3b,c). After 1 h of polymerization, a progressive decrease in d_{edge} with increasing [EBiB] was observed (Figures 3c and S7), and this was mirrored by a concomitant reduction in T_{dry} (Figure 3b). Efficient trapping of O_2 by radicals generated in solution led to a gradual reduction in brush-growth inhibition at the edges of the substrates. This was achieved at the expense of a brush-thickening rate. The increase in the content of EBiB and the consequent termination of generated radicals upon recombination with O_2 altered the ATRP equilibrium and led to an accumulation of Cu^{II}-based deactivators. This phenomenon caused a progressive slowing down of the polymerization rate from the surface and thus the generation of thinner brushes.

When [$CuBr_2$/Me_6TREN] was decreased to 0.5 mM, the addition of EBiB in solution had a more marked effect on d_{edge}, which decreased by ∼0.8 mm for [EBiB] = 1 mM, compared to brush films synthesized without a sacrificial initiator (Figures 3b,c and S8). Interestingly, for [$CuBr_2$/Me_6TREN] = 0.5 mM, T_{dry} showed a slight increase, reaching a maximum for [EBiB] = 0.1 mM, while a further increment in the content of the sacrificial initiator was accompanied by a significant decrease in brush thickness (Figure 3b). Relevant to this, a marked drop in d_{edge} recorded at [EBiB] = 0.1 mM corresponded to the maximum value of T_{dry}. These observed trends suggested that variations in [EBiB] contributed in different ways to oxygen consumption and deactivation during SI-photoATRP. On the one hand, with [EBiB] ≤ 0.1 mM, radical generation in solution was sufficient to improve oxygen consumption without determining the significant effects on activation/deactivation processes and polymerization rate. On the other hand, for [EBiB] > 0.1 mM, the increase in the relative content of the Cu^{II}-based deactivator provided lower brush-growth rates, while tolerance toward O_2 was markedly enhanced by the high concentration of radicals in solution.

The effect of confinement on the tolerance of SI-photoATRP toward oxygen was finally investigated. Typical SI-photoATRP setups featured extremely small reaction volumes (*i.e.*, a distance between initiator-bearing substrate and the confining glass cover, *z*, of ∼10 μm, Figure S1 and Figure 4). In such highly confined volumes, deoxygenation of polymerization mixtures can be avoided, and the growth of brushes is only hampered at the edges of the substrates by oxygen diffusing from the surrounding environment.[21,38]

In the absence of confinement, by increasing *z*, tolerance toward O_2 is compromised due to the increase in the area at the sides of the substrate through which oxygen can freely diffuse into the reaction medium. This phenomenon significantly limits the applicability of SI-photoATRP within large-scale settings. However, although reaction volumes are increased, resistance toward diffusing O_2 could be (re)gained by adding a sacrificial initiator within the polymerization mixture, which compensates for the increment in oxygen concentration with a concomitant increase in scavenging radical species generated in solution.

In order to evaluate confinement effects on SI-photoATRP with and without a sacrificial initiator, larger substrates (25 × 75 mm^2) were employed together with glass spacers presenting different thicknesses (*z* = 0.10, 0.15, and 0.18 mm), which were positioned between the confining glass cover and the initiating surfaces (Figure S2 and Figure 4). The composition of the polymerization mixtures was kept constant (5 mM $CuBr_2$ and 30 mM Me_6TREN), except when EBiB was introduced in the system, while polymerization time was set to 1 h.

In the absence of a sacrificial initiator, T_{dry} decreased with increasing reaction volume, *i.e.*, while increasing *z*, due to the fastest diffusion of O_2 within a less-confined polymerization setup, reaching 27.4 ± 0.1 nm when *z* was set at the largest value of 0.18 ± 0.02 mm (Figure 5a). This corresponded to more than a 2-fold decrease in T_{dry} when compared to the value recorded for the sample presenting the highest degree of confinement ("quasi-contact", *z* ∼ 10 μm). At the same time, d_{edge} increased progressively from 3.0 ± 0.5 mm to 4.2 ± 0.5 mm (Figure 5b) due to a more pronounced recombination of propagating radicals with O_2.

The presence of a sacrificial initiator in solution provided a source of radicals that could promptly recombine with O_2, suppressing termination of surface-grafted propagating chains. Addition of 1 mM EBiB as the sacrificial initiator while keeping

https://doi.org/10.1021/acsmacrolett.3c00359
ACS Macro Lett. 2023, 12, 1166−1172

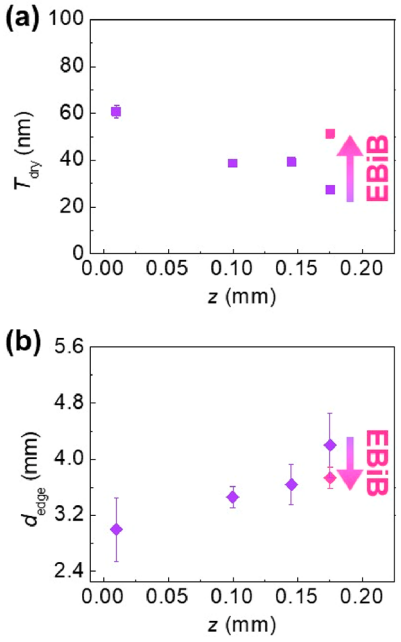

Figure 5. (a) Dry thickness (T_{dry}) and (b) edge distance (d_{edge}) as a function of spacers' height (z) in SI-photoATRP of OEGMA (M_n ~ 300 Da) carried out in polymerization mixtures comprising 1:1 (v/v) DMF:OEGMA, 5 mM $CuBr_2$, and 30 mM Me_6TREN. Polymerizations were performed under different degrees of confinement and in the absence/presence of 1 mM EBiB as the sacrificial initiator.

z = 0.18 ± 0.02 mm provided brushes with T_{dry} = 51.3 ± 0.2 nm, which was just 16% lower than the brush thickness obtained by performing SI-photoATRP within highly confined environments (Figures 5a and S9). Simultaneously, the presence of a sacrificial initiator caused a reduction of d_{edge} by ~0.5 mm with respect to the values recorded at the same z but without EBiB (Figure 5b). Hence, these findings demonstrated that the introduction of a sacrificial initiator improved oxygen tolerance of SI-photoATRP, even when brush coatings were fabricated within a less confined space.

The influence of a variation in confinement can be visualized in one substrate by performing SI-photoATRP while varying z through tilting of the confining cover surface, i.e., varying z from ~50 μm to 0.18 ± 0.02 mm over a ~4 cm wide initiating substrate (Figure 6a). By applying a polymerization mixture comprising 5 mM $CuBr_2$ and 30 mM Me_6TREN, after 60 min of UV irradiation, a POEGMA brush gradient was obtained, featuring T_{dry} ranging from 57.4 ± 0.6 nm (z ~ 50 μm) to 37 ± 2 nm (z ~ 0.18 cm; Figure 6b, black squares). On the areas of the substrate where z became relatively large, brush growth was significantly inhibited by diffusing O_2. It is relevant that when 1 mM EBiB was added to the polymerization mixture and the reaction time was kept constant, POEGMA brushes showing uniform T_{dry} across the entire substrate were obtained by employing an otherwise identical setup (Figure 6b, yellow squares).

In summary, we demonstrated that the tolerance of SI-photoATRP toward environmental conditions can be finely modulated by varying the composition of the polymerization mixture and the setup employed for fabricating polymer brushes. While an increment in the concentration of Cu-based catalyst influences the consumption of O_2 present in the reaction mixture and diffusing to it from the surrounding environment, a more marked effect by the presence of sacrificial initiator in solution was clearly identified. Radicals generated in the medium thus emerge as a key component that can quickly recombine with oxygen and suppress the termination of brush-growth by O_2 at the edges of substrates, finally providing uniformly functionalized surfaces. This is also valid when confinement of polymerization is reduced, *i.e.*, when the distance between the confining glass covers and the initiating substrates is increased, enabling the efficient growth of thick brushes within more accessible and practical setups.

This study contributes to our previous efforts in identifying the main processes that could enable the translation of SI-ATRP techniques into technologically relevant settings, and highlights how photochemical SI-RDRPs could realistically turn into scalable surface fabrications.

■ ASSOCIATED CONTENT

Supporting Information

The Supporting Information is available free of charge at https://pubs.acs.org/doi/10.1021/acsmacrolett.3c00359.

Employed materials and equipment, experimental procedures, additional figures, and photographs of the brush-functionalized substrates (PDF)

■ AUTHOR INFORMATION

Corresponding Authors

Krzysztof Matyjaszewski − *Department of Chemistry, Carnegie Mellon University, Pittsburgh, Pennsylvania 15213,*

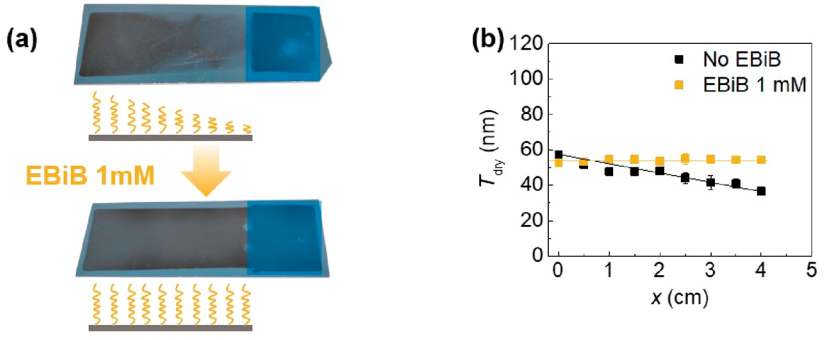

Figure 6. (a) Effect of the addition of 1 mM EBiB as a sacrificial initiator in SI-photoATRP of OEGMA (M_n ~ 300 Da) carried out varying z along the substrate. (b) Variation of brush dry thickness (T_{dry}) along the substrate, from one extremity (x = 0) to the spacer (x = 4 cm, spacer thickness z = 0.18 ± 0.02 mm), for the SI-photoATRP of OEGMA (M_n ~ 300 Da) carried out in polymerization mixtures comprising 1:1 (v/v) DMF:OEGMA, 5 mM $CuBr_2$, and 30 mM Me_6TREN, in the absence and presence of 1 mM EBiB.

https://doi.org/10.1021/acsmacrolett.3c00359
ACS Macro Lett. 2023, 12, 1166−1172

United States; orcid.org/0000-0003-1960-3402; Email: km3b@andrew.cmu.edu

Francesca Lorandi − *Laboratory for Macromolecular and Organic Chemistry, Department of Chemical Sciences, University of Padova, 35131 Padova, Italy*; orcid.org/0000-0001-5253-8468; Email: francesca.lorandi@unipd.it

Edmondo M. Benetti − *Laboratory for Macromolecular and Organic Chemistry, Department of Chemical Sciences, University of Padova, 35131 Padova, Italy*; orcid.org/0000-0002-5657-5714; Email: edmondo.benetti@unipd.it

Authors

Gianluca Gazzola − *Laboratory for Macromolecular and Organic Chemistry, Department of Chemical Sciences, University of Padova, 35131 Padova, Italy*

Irene Filipucci − *Laboratory for Macromolecular and Organic Chemistry, Department of Chemical Sciences, University of Padova, 35131 Padova, Italy*

Andrea Rossa − *Laboratory for Macromolecular and Organic Chemistry, Department of Chemical Sciences, University of Padova, 35131 Padova, Italy*; orcid.org/0000-0002-8316-4646

Complete contact information is available at: https://pubs.acs.org/10.1021/acsmacrolett.3c00359

Author Contributions

CRediT: **Gianluca Gazzola** data curation (equal), formal analysis (equal), methodology (equal), writing-original draft (equal); **Irene Filipucci** data curation (equal), investigation (equal), methodology (equal); **Andrea Rossa** data curation (equal), methodology (equal), validation (equal); **Krzysztof Matyjaszewski** project administration (supporting), supervision (supporting), writing-original draft (supporting), writing-review & editing (supporting); **Francesca Lorandi** project administration (supporting), supervision (supporting), writing-original draft (supporting); **Edmondo M. Benetti** conceptualization (lead), funding acquisition (lead), project administration (lead), supervision (lead), writing-original draft (lead), writing-review & editing (lead).

Notes

The authors declare no competing financial interest.

■ ACKNOWLEDGMENTS

G.G. acknowledges financial support by the Italian Ministry of Research and University (MUR), through PNRR DM 352/2022 (C96E22000200005); E.M.B. and F.L. acknowledge support from the Nanochemistry for Energy and Health (NEXUS) "Department of Excellence" program by the Department of Chemical Sciences of the University of Padova. K.M. acknowledges support from NSF (CHE 2000391). We are grateful to Dr. Ilaria Fortunati for the technical support.

■ REFERENCES

(1) Yeow, J.; Chapman, R.; Gormley, A. J.; Boyer, C. Up in the air: oxygen tolerance in controlled/living radical polymerisation. *Chem. Soc. Rev.* **2018**, *47* (12), 4357−4387.

(2) Dolinski, N. D.; Page, Z. A.; Discekici, E. H.; Meis, D.; Lee, I. H.; Jones, G. R.; Whitfield, R.; Pan, X.; McCarthy, B. G.; Shanmugam, S.; et al. What happens in the dark? Assessing the temporal control of photo-mediated controlled radical polymerizations. *J. Polym. Sci., Part A: Polym. Chem.* **2019**, *57* (3), 268−273.

(3) Fromel, M.; Benetti, E. M.; Pester, C. W. Oxygen tolerance in surface-initiated reversible deactivation radical polymerizations: Are polymer brushes turning into technology? *ACS Macro Lett.* **2022**, *11* (4), 415−421.

(4) Corrigan, N.; Jung, K.; Moad, G.; Hawker, C. J.; Matyjaszewski, K.; Boyer, C. Reversible-deactivation radical polymerization (Controlled/living radical polymerization): From discovery to materials design and applications. *Prog. Polym. Sci.* **2020**, *111*, 101311.

(5) Sato, T.; Dunderdale, G. J.; Urata, C.; Hozumi, A. Sol−Gel Preparation of initiator layers for surface-initiated ATRP: large-scale formation of polymer brushes is not a dream. *Macromolecules* **2018**, *51* (24), 10065−10073.

(6) Joh, D. Y.; Hucknall, A. M.; Wei, Q.; Mason, K. A.; Lund, M. L.; Fontes, C. M.; Hill, R. T.; Blair, R.; Zimmers, Z.; Achar, R. K.; et al. Inkjet-printed point-of-care immunoassay on a nanoscale polymer brush enables subpicomolar detection of analytes in blood. *Proc. Natl. Acad. Sci. U.S.A.* **2017**, *114* (34), E7054−E7062.

(7) Zoppe, J. O.; Ataman, N. C.; Mocny, P.; Wang, J.; Moraes, J.; Klok, H.-A. Surface-Initiated Controlled Radical Polymerization: State-of-the-Art, Opportunities, and Challenges in Surface and Interface Engineering with Polymer Brushes. *Chem. Rev.* **2017**, *117* (3), 1105−1318.

(8) Matyjaszewski, K.; Dong, H.; Jakubowski, W.; Pietrasik, J.; Kusumo, A. Grafting from surfaces for "everyone": ARGET ATRP in the presence of air. *Langmuir* **2007**, *23* (8), 4528−4531.

(9) Hong, D.; Hung, H.-C.; Wu, K.; Lin, X.; Sun, F.; Zhang, P.; Liu, S.; Cook, K. E.; Jiang, S. Achieving ultralow fouling under ambient conditions via surface-initiated ARGET ATRP of carboxybetaine. *ACS Appl. Mater. Interfaces* **2017**, *9* (11), 9255−9259.

(10) Kang, H.; Jeong, W.; Hong, D. Antifouling surface coating using droplet-based SI-ARGET ATRP of carboxybetaine under open-air conditions. *Langmuir* **2019**, *35* (24), 7744−7750.

(11) Dunderdale, G. J.; Urata, C.; Miranda, D. F.; Hozumi, A. Large-scale and environmentally friendly synthesis of pH-responsive oil-repellent polymer brush surfaces under ambient conditions. *ACS Appl. Mater. Interfaces* **2014**, *6* (15), 11864−11868.

(12) Zhang, T.; Du, Y.; Kalbacova, J.; Schubel, R.; Rodriguez, R. D.; Chen, T.; Zahn, D. R.; Jordan, R. Wafer-scale synthesis of defined polymer brushes under ambient conditions. *Polym. Chem.* **2015**, *6* (47), 8176−8183.

(13) Dehghani, E. S.; Du, Y.; Zhang, T.; Ramakrishna, S. N.; Spencer, N. D.; Jordan, R.; Benetti, E. M. Fabrication and interfacial properties of polymer brush gradients by surface-initiated Cu (0)-mediated controlled radical polymerization. *Macromolecules* **2017**, *50* (6), 2436−2446.

(14) Che, Y.; Zhang, T.; Du, Y.; Amin, I.; Marschelke, C.; Jordan, R. On Water" Surface-initiated Polymerization of Hydrophobic Monomers. *Angew. Chem., Int. Ed.* **2018**, *57* (50), 16380−16384.

(15) Fantin, M.; Ramakrishna, S. N.; Yan, J.; Yan, W.; Divandari, M.; Spencer, N. D.; Matyjaszewski, K.; Benetti, E. M. The Role of Cu0 in Surface-Initiated Atom Transfer Radical Polymerization: Tuning Catalyst Dissolution for Tailoring Polymer Interfaces. *Macromolecules* **2018**, *51* (17), 6825−6835.

(16) Yan, W.; Fantin, M.; Spencer, N. D.; Matyjaszewski, K.; Benetti, E. M. Translating surface-initiated atom transfer radical polymerization into technology: The mechanism of Cu0-mediated si-atrp under environmental conditions. *ACS Macro Lett.* **2019**, *8* (7), 865−870.

(17) Zhang, T.; Benetti, E. M.; Jordan, R. Surface-Initiated Cu(0)-Mediated CRP for the Rapid and Controlled Synthesis of Quasi-3D Structured Polymer Brushes. *ACS Macro Lett.* **2019**, *8* (2), 145−153.

(18) Layadi, A.; Kessel, B.; Yan, W.; Romio, M.; Spencer, N. D.; Zenobi-Wong, M.; Matyjaszewski, K.; Benetti, E. M. Oxygen tolerant and cytocompatible Iron (0)-mediated ATRP enables the controlled growth of polymer brushes from mammalian cell cultures. *J. Am. Chem. Soc.* **2020**, *142* (6), 3158−3164.

(19) Albers, R. F.; Yan, W.; Romio, M.; Leite, E. R.; Spencer, N. D.; Matyjaszewski, K.; Benetti, E. M. Mechanism and application of surface-initiated ATRP in the presence of a Zn 0 plate. *Polym. Chem.* **2020**, *11* (44), 7009−7014.

(20) Navarro, L. A.; Enciso, A. E.; Matyjaszewski, K.; Zauscher, S. Enzymatically Degassed Surface-Initiated Atom Transfer Radical Polymerization with Real-Time Monitoring. *J. Am. Chem. Soc.* **2019**, *141* (7), 3100−3109.
(21) Yan, W.; Dadashi-Silab, S.; Matyjaszewski, K.; Spencer, N. D.; Benetti, E. M. Surface-initiated photoinduced ATRP: Mechanism, oxygen tolerance, and temporal control during the synthesis of polymer brushes. *Macromolecules* **2020**, *53* (8), 2801−2810.
(22) Ribelli, T. G.; Konkolewicz, D.; Bernhard, S.; Matyjaszewski, K. How are radicals (re) generated in photochemical ATRP? *J. Am. Chem. Soc.* **2014**, *136* (38), 13303−13312.
(23) Bondarev, D.; Borská, K.; Šoral, M.; Moravčíková, D.; Mosnáček, J. Simple tertiary amines as promotors in oxygen tolerant photochemically induced ATRP of acrylates. *Polymer* **2019**, *161*, 122−127.
(24) Marathianos, A.; Liarou, E.; Anastasaki, A.; Whitfield, R.; Laurel, M.; Wemyss, A. M.; Haddleton, D. M. Photo-induced copper-RDRP in continuous flow without external deoxygenation. *Polym. Chem.* **2019**, *10* (32), 4402−4406.
(25) Narupai, B.; Page, Z. A.; Treat, N. J.; McGrath, A. J.; Pester, C. W.; Discekici, E. H.; Dolinski, N. D.; Meyers, G. F.; Read de Alaniz, J.; Hawker, C. J. Simultaneous preparation of multiple polymer brushes under ambient conditions using microliter volumes. *Angew. Chem., Int. Ed.* **2018**, *57* (41), 13433−13438.
(26) Discekici, E. H.; Pester, C. W.; Treat, N. J.; Lawrence, J.; Mattson, K. M.; Narupai, B.; Toumayan, E. P.; Luo, Y.; McGrath, A. J.; Clark, P. G.; et al. Simple benchtop approach to polymer brush nanostructures using visible-light-mediated metal-free atom transfer radical polymerization. *ACS Macro Lett.* **2016**, *5* (2), 258−262.
(27) Li, M.; Fromel, M.; Ranaweera, D.; Rocha, S.; Boyer, C.; Pester, C. W. SI-PET-RAFT: surface-initiated photoinduced electron transfer-reversible addition−fragmentation chain transfer polymerization. *ACS Macro Lett.* **2019**, *8* (4), 374−380.
(28) Rolland, M.; Whitfield, R.; Messmer, D.; Parkatzidis, K.; Truong, N. P.; Anastasaki, A. Effect of polymerization components on Oxygen-Tolerant Photo-ATRP. *ACS Macro Lett.* **2019**, *8* (12), 1546−1551.
(29) Anastasaki, A.; Nikolaou, V.; Zhang, Q.; Burns, J.; Samanta, S. R.; Waldron, C.; Haddleton, A. J.; McHale, R.; Fox, D.; Percec, V.; et al. Copper (II)/tertiary amine synergy in photoinduced living radical polymerization: Accelerated synthesis of ω-functional and α, ω-heterofunctional poly (acrylates). *J. Am. Chem. Soc.* **2014**, *136* (3), 1141−1149.
(30) Frick, E.; Anastasaki, A.; Haddleton, D. M.; Barner-Kowollik, C. Enlightening the mechanism of copper mediated photoRDRP via high-resolution mass spectrometry. *J. Am. Chem. Soc.* **2015**, *137* (21), 6889−6896.
(31) Mosnáček, J.; Eckstein-Andicsova, A.; Borska, K. Ligand effect and oxygen tolerance studies in photochemically induced copper mediated reversible deactivation radical polymerization of methyl methacrylate in dimethyl sulfoxide. *Polym. Chem.* **2015**, *6* (13), 2523−2530.
(32) Borská, K.; Moravčíková, D.; Mosnáček, J. Photochemically induced ATRP of (meth) acrylates in the presence of air: the effect of light intensity, ligand, and oxygen concentration. *Macromol. Rapid Commun.* **2017**, *38* (13), 1600639.
(33) Parkatzidis, K.; Truong, N. P.; Whitfield, R.; Campi, C. E.; Grimm-Lebsanft, B.; Buchenau, S.; Rübhausen, M. A.; Harrisson, S.; Konkolewicz, D.; Schindler, S.; Anastasaki, A. Oxygen-Enhanced Atom Transfer Radical Polymerization through the Formation of a Copper Superoxido Complex. *J. Am. Chem. Soc.* **2023**, *145* (3), 1906−1915.
(34) Dadashi-Silab, S.; Lee, I.-H.; Anastasaki, A.; Lorandi, F.; Narupai, B.; Dolinski, N. D.; Allegrezza, M. L.; Fantin, M.; Konkolewicz, D.; Hawker, C. J.; Matyjaszewski, K. Investigating Temporal Control in Photoinduced Atom Transfer Radical Polymerization. *Macromolecules* **2020**, *53* (13), 5280−5288.
(35) Matyjaszewski, K.; Miller, P. J.; Shukla, N.; Immaraporn, B.; Gelman, A.; Luokala, B. B.; Siclovan, T. M.; Kickelbick, G.; Vallant, T.; Hoffmann, H.; et al. Polymers at interfaces: using atom transfer radical polymerization in the controlled growth of homopolymers and block copolymers from silicon surfaces in the absence of untethered sacrificial initiator. *Macromolecules* **1999**, *32* (26), 8716−8724.
(36) Kang, C.; Crockett, R. M.; Spencer, N. D. Molecular-weight determination of polymer brushes generated by SI-ATRP on flat surfaces. *Macromolecules* **2014**, *47* (1), 269−275.
(37) Wang, R.; Wei, Q.; Sheng, W.; Yu, B.; Zhou, F.; Li, B. Driving Polymer Brushes from Synthesis to Functioning. *Angew. Chem.* **2023**, *135*, e202219312.
(38) Benetti, E. M.; Kang, C.; Mandal, J.; Divandari, M.; Spencer, N. D. Modulation of surface-initiated ATRP by confinement: Mechanism and applications. *Macromolecules* **2017**, *50* (15), 5711−5718.

https://doi.org/10.1021/acsmacrolett.3c00359
ACS Macro Lett. 2023, 12, 1166−1172